Linear analysis of wave basins and absorbers

by J. N. Newman
<jnn@mit.edu>

Wave basins are usually equipped with banks of wavemakers on one or two sides, and beaches on the opposite sides. Most wavemakers are oscillatory in rotational ('hinged-flap') or translational ('piston') modes. As an alternative to conventional beaches, wavemakers with active controls can be used as absorbers [1,2,3]. Absorbers have the advantages that they do not extend into the experimental domain of the basin and, at least in linear theory, low or zero reflection can be achieved. In order to generate and absorb plane waves at oblique angles, or more general three-dimensional wave systems, it is necessary to use a large number of wavemakers with small widths compared to the wavelength [4].

Wavemakers and absorbers are usually analyzed with Havelock's theory [5], which applies to a semi-infinite fluid domain. A radiation condition is imposed, and each wavemaker radiates waves which propagate to infinity. As in the case of a floating body in an infinite fluid, the hydrodynamic pressure force includes both added-mass and damping components. This approach is intuitively logical if the horizontal scale of the basin is large compared to the wavelength, and if reflections are ignored.

It is more rational to consider the basin as a finite domain, but this changes the linear inviscid theory in a fundamental manner. The waves are reflected on the basin walls, and there is no energy radiation. Considering each wavemaker mode separately, and assuming steady-state harmonic time dependence, standing waves are generated and the fluid velocity throughout the basin is in phase with the wavemaker. There is no wave damping, only an added-mass component of the pressure force.

Progressive waves can be generated in a finite basin by combining different wavemaker modes with appropriate phase differences. In the simplest case of two dimensions, with identical wavemakers at the ends $x = 0$ and $x = L$, if the wavemaker at $x = 0$ oscillates with amplitude $\mathrm{Re}\,\xi_1 \mathrm{e}^{\mathrm{i}\omega t}$, outgoing waves of the form $\zeta = \mathrm{Re}\,\xi_1 C \mathrm{e}^{\mathrm{i}(\omega t - kx)}$ are generated before accounting for reflections. Here C is a complex constant. The reflection of this wave system can be cancelled by the second wavemaker, at $x = L$, if its amplitude is $\xi_2 = -\xi_1 \mathrm{e}^{-\mathrm{i}kL}$. The combined result of these two wavemaker motions is a progressive wave moving in the $+x$-direction, except for the evanescent field close to each wavemaker. If $-\omega^2 A_{ij}$ denotes the added-mass force acting on wavemaker i due to the motion of wavemaker j with unit amplitude, the forces acting on the two wavemakers are $-\omega^2 \xi_1 (A_{11} - \mathrm{e}^{-\mathrm{i}kL} A_{12})$ and $-\omega^2 \xi_2 (A_{22} - \mathrm{e}^{\mathrm{i}kL} A_{21})$. Since $A_{11} = A_{22}$ and $A_{12} = A_{21}$, the 'effective' added mass of each wavemaker is $(A_{11} - A_{12} \cos kL)$ and the 'effective' damping coefficients are $\mp A_{12} \sin kL$. (For $kL >> 1$ it follows from the usual eigenfunction expansion that $A_{12} \sin kL < 0$. Thus the damping is positive for the first wavemaker and negative for the second wavemaker, as expected.)

This provides a connection between the added-mass matrix for two wavemakers in a finite basin and the effective added mass plus damping for a single wavemaker. (We exclude eigenfrequencies of the basin, where $\sin kL = 0$.) The individual added-mass coefficients A_{ij} are oscillatory functions of kL, which tend to $\pm\infty$ at the eigenfrequencies. However the 'effective' added mass and damping defined above are bounded, and tend to the non-oscillatory limits derived from Havelock's theory if $kL >> 1$.

The three-dimensional case can be analyzed numerically, using either separation of variables and eigenfunction expansions for simple geometries or a more general radiation-diffraction code. The results shown here have been computed using WAMIT. Two specific cases are considered, a square basin 16 m by 16 m by 1 m depth, and a round basin of radius 10 m and depth 1 m. Hinged-flap wavemakers are distributed uniformly around the periphery, with the hinges at the bottom. The generating wavemakers for the square basin are on two adjacent sides, as shown by the black rectangles in Figures 1-4, and the absorbing wavemakers (red) are on the two opposite sides. For the round basin the generating and absorbing wavemakers occupy opposite semi-circular segments, as shown in Figure 5. Except where otherwise noted, the normal velocity of each wavemaker (both generating and absorbing) is equal to the normal component of the orbital velocity of a progressive wave at the center of the wavemaker; this is referred to below as 'kinematic' absorption.

The results shown in Figures 1-5 are for a period of 2 seconds, corresponding to a wavelength of 5.2 m. Contour plots are shown of the wave amplitude over the free surface, excluding a 1 m strip adjacent to the wavemakers. For pure progressive waves the amplitude is constant. Reflections and other imperfections in the generated wave system are indicated by fluctuations of the amplitude. The magnitude of the fluctuations is measured in each plot by the standard deviation σ, defined as the square-root of the variance normalized by the mean value.

Figure 1 shows the waves in the square tank without absorption, at incidence angles $\beta = 0$ and 30 degrees relative to the $+x$-axis. In the case $\beta = 0$ a two-dimensional standing wave is present. For $\beta = 30°$ the standing-wave system is three-dimensional. Figure 2 shows the corresponding results with kinematic absorption. The left figure ($\beta = 0$) indicates almost perfect absorption with $\sigma = 0.002$. For nonzero incidence angles the standard deviation is larger, due to the finite width of the wavemakers. For these results a total of 128 wavemakers are used, with a width of 0.5 m.

Figure 3 shows the effect of using 64 wavemakers (left) of width 1 m or 256 0.25 m wavemakers (right). As expected, the amplitude fluctuations for oblique waves can be reduced by decreasing the width of each wavemaker, and conversely. These results suggest that the standard deviation is more-or-less proportional to the square of the wavemaker width.

In order to improve the utility of absorbing wavemakers it is necessary to avoid an *a priori* specification of the amplitude and phase, so that other waves can be absorbed including those radiated and diffracted from bodies in the basin. In experimental applications it is customary to measure either the incoming waves before they reach the wavemaker, as in [1], or the hydrodynamic force acting on the wavemaker, as discussed in [2] and [3], and use this to optimize the absorber controls. Using the measured force on the wavemaker is advantageous, especially in two dimensions or with normally incident waves. Results to illustrate this situation are shown in Figure 4. Each absorber's motion is determined by a coupled equation of motion with external damping equal to the effective wave damping coefficient, and an external inertial restraint equal to the negative of the effective added mass. This 'dynamic' control system gives perfect absorption if the waves are normally incident upon the absorber, but in other cases it is less effective. The latter problem is most evident in the case $\beta = 0$, shown on the left in Figure 4, where the waves propagate in the direction parallel to the lower right wall; ideally the absorbers along this wall should be stationary, but instead they react to the pressure of the passing wave system to extract energy.

Figure 5 shows the wave amplitude in the round basin. In the upper figure the absorbers are stationary and three-dimensional standing waves are generated. In the lower figures the waves propagate in the $+y$-direction and the absorbers are kinematic (left) or dynamic (right).

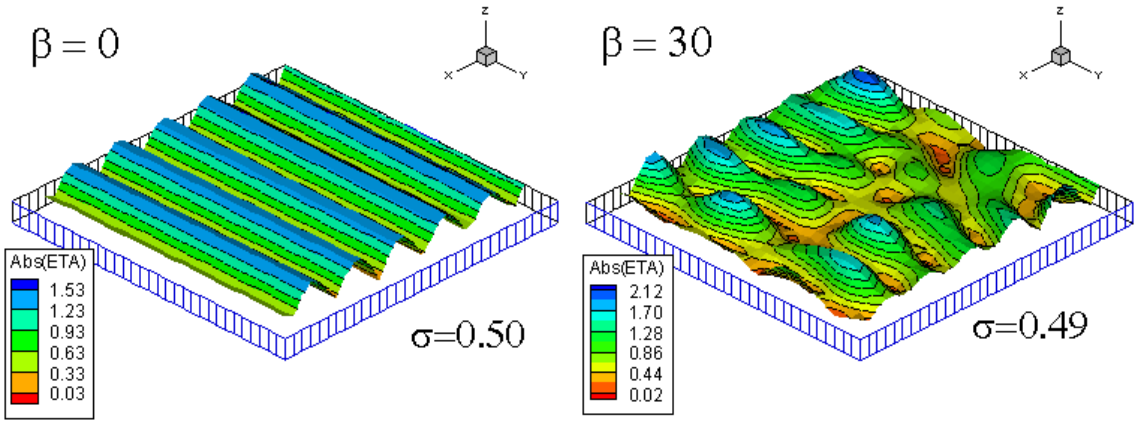

Figure 1: Amplitude of standing waves generated in the square basin with stationary wave absorbers, at angles $\beta = 0$ (left) and $\beta = 30°$ (right). 128 wavemakers with width 0.5 m are used, including both generators (black) and absorbers (red). Note that different ranges of colors are used to represent the amplitude in each plot.

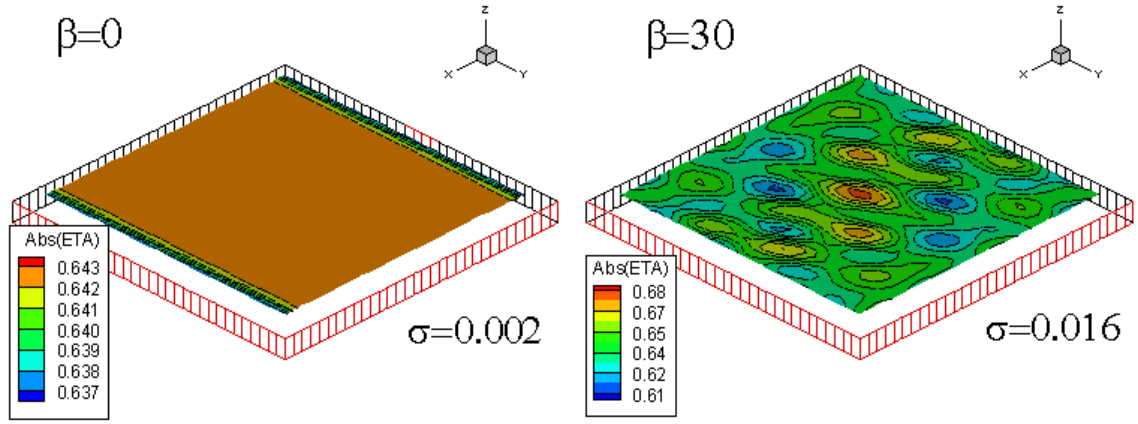

Figure 2: Amplitude of progressive waves with kinematic absorbers at $\beta = 0$ (left) and $\beta = 30°$ (right).

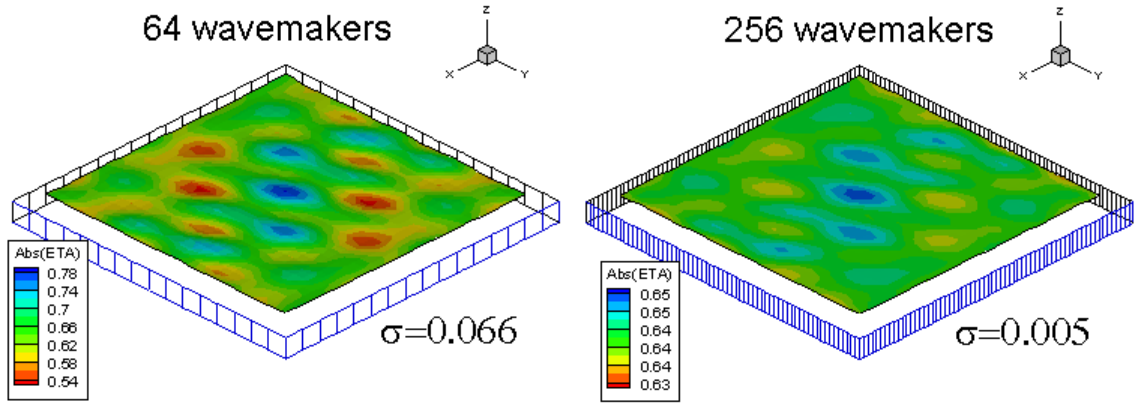

Figure 3: Amplitude of progressive waves with kinematic absorbers at the incidence angle $\beta = 30°$, showing the effect of the number of wavemakers. (These should be compared with the right plot in Figure 2, where 128 wavemakers are used.)

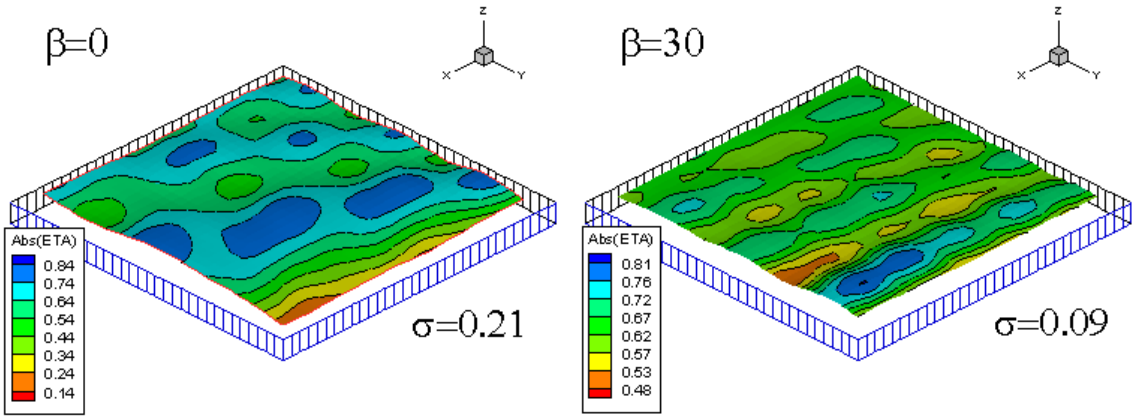

Figure 4: Amplitude of progressive waves with dynamic absorption at $\beta = 0$ (left) and $\beta = 30°$ (right).

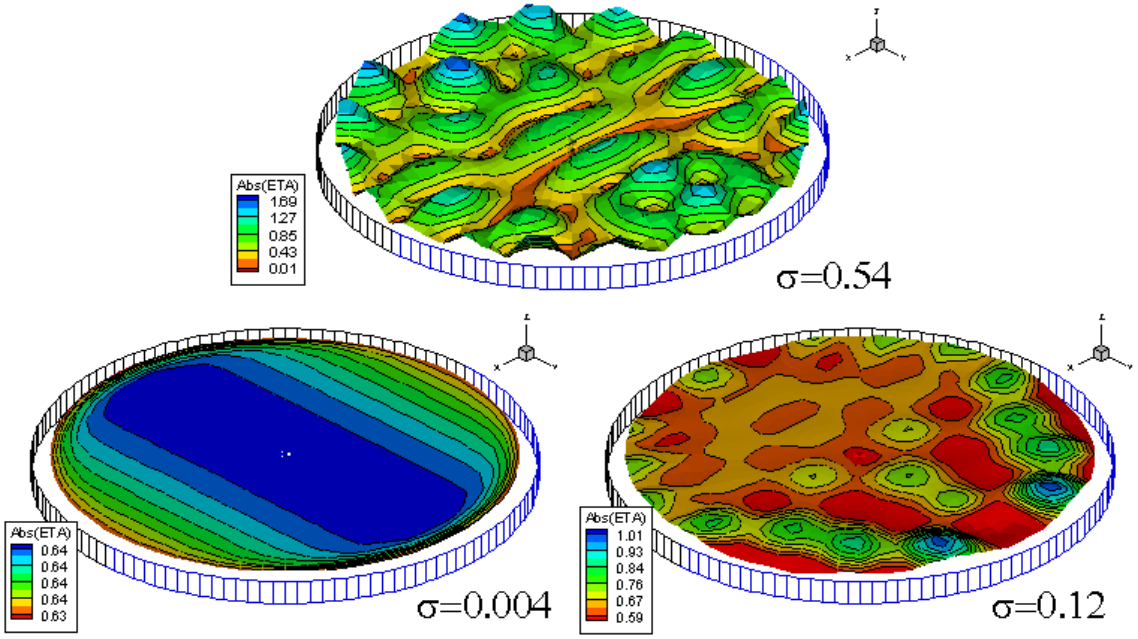

Figure 5: Wave amplitude in the round basin, with generators (black) in the sector ($y < 0$) and absorbers (red) in ($y > 0$). The upper plot shows the standing wave system without absorption. The lower plots show the amplitude of waves propagating in the $+y$-direction with kinematic (left) and dynamic (right) absorbers.

References

[1] Milgram, J. 'Active water-wave absorbers,' J. Fluid Mech. **43**, 845-859, 1970.

[2] Salter, S. H. 'Absorbing wave-makers and wide tanks,' Proc. Directional Wave Spectra Applications, Berkeley, 1981.

[3] Naito, S. 'Wave generation and absorption in wave basins: theory and application,' J. ISOPE, **16**, 2, 81-89, 2006.

[4] O'Dea, J.F. and Newman, J.N., 'Numerical studies of directional wavemaker performance,' 28th American Towing Tank Conference, Ann Arbor, Michigan 2007.

[5] Havelock, T. H. 'Forced surface waves on water,' Phil. Mag. **8**, 569-576, 1929.